Compressive sensing method to leverage prior information for submerged target echoes

Tongjing Sun [1*], Philippe Blondel [2], Bing Jia [3], Guijuan Li [3], Enwei Gao [1]

[1]*Department of Automation, Hangzhou Dianzi University, Xiasha Higher Education Zone, Hangzhou, 310018, China*

[2]*Department of Physics, University of Bath, Claverton Down, Bath, BA2 7AY, United Kingdom*

[3]*Underwater Test & Control Technology Key Laboratory, No. 14 Binhai Street Zhongshan Zone, Dalian, 116013, China*

** Corresponding author: stj@hdu.edu.cn*

Abstract: *Reducing data volume and improving signal-to-noise ratio (SNR) is of great importance for echoes from submerged targets, affected by serious marine environment noise. The echo from a target is made of its response to the incident wave, with the superposition of highlights (sub-echoes from main constituents of the target). Each of these highlights can be seen as a block, and the echo therefore has a block-sparse feature. This paper proposes a Compressive Sensing method to leverage Prior Information (CSPI), in which knowledge of the incident wave and the block-sparse feature are leveraged into the dictionary structure and signal reconstruction. CSPI is illustrated with simulations and field measurements of backscattering for a 1:20 model of the Benchmark Target Strength Simulation Submarine (BeTSSi-Sub). CSPI performance is verified by analyzing the matching rate and signal-to-noise ratio (SNR). For simulated signals with different noise levels, CSPI can increase the matching rate, reconstruct an almost invisible signal (original SNR = 0 dB), and improve SNR by up to 13dB (for an original SNR of 4 dB) down to a still significant SNR of 7 dB (for an original SNR of 0 dB). For field measurements, CSPI can obtain the same SNR as the original signal using only 13% of the data, increasing SNR to 15 dB using 30% data, and increasing with the compression ratio.*

I. Introduction

Ocean environments are complex and highly changeable, both in time and in space. With low signal levels, in particular after propagation over significant ranges, echoes from underwater targets will often have low signal-to-noise ratio (SNR). This brings serious challenges to active sonar detection and recognition. In recent years, researchers have investigated the fine structures of acoustic scattering from targets by using theoretical[1] and experimental[2]-[4] methods. Additional efforts have borne on active sonar echo signal processing methods[5][6] and the use of different incident signals[7][8]. At present, broadband systems[9][10] are an effective way to improve SNR and detection performance. However, they produce very large amounts of data, bringing heavy burdens to data acquisition, storage, transmission and processing[11]. Therefore, improving SNR without increasing the amount of data, or even whilst reducing the amount of data, became a pressing problem in active sonar detection and identification of target echoes.

The new research field of Compressive Sensing (CS)[12]-[14] is based on sparse signal representation and approximation theory. It makes full use of the signals' sparse characteristics, projecting high-dimensional sparse signals to low-dimensional space with a random matrix, and then reconstructing the original signal with high-fidelity by solving an optimization problem from these few projections. CS theory breaks the constraints of the traditional Nyquist sampling theorem, affording the detection of unknown signals and their compression at the same time. Under certain conditions, only a small amount of data requires to be sampled, and the original signal can be recovered precisely from the reconstruction algorithm. Because of low sampling rates and highly accurate recovery data, this technique has been widely used in data collection[15]-[16], medical imaging[17]-[19], radar[20]-[22], and communications[23]-[25].

Applications of CS to underwater echoes mainly include signal compression and reconstruction[26], acoustic signal processing[27]-[29], and target classification and recognition[30]-[32]. For example[26], a Gaussian random matrix is used as the measurement matrix, and an orthogonal matching pursuit algorithm is used to realize the compression and reconstruction of acoustic data. Discrete Cosine Transform (DCT) has also been used[30][31] for signal decomposition, and for sparse reconstruction and recognition of underwater signals and target echoes. Other applications[32] have used an echo training sample set as a dictionary to classify acoustic returns from targets. CS is also used to process and analyze the data from acoustic arrays, and some studies[27] have shown the improvements of SNR by 12 dB compared to 8 dB with traditional beamforming. Most of these previous studies did not consider prior information using DCT or training method to form the dictionary necessary for CS. According to one of its basic properties, the closer the atomic property in the dictionary is to the original signal, the better are the results of compressive sensing and reconstruction. Therefore, making full use of prior information[33] is an effective way to improve the performance of CS.

In this paper, in order to improve SNR and reduce the amount of data, a priori information is integrated into the dictionary structure and reconstruction algorithm based on the active sonar echo signal principle and waveform characteristics. Compressive Sensing using Prior Information (CSPI) is introduced in section II. The performance of this approach is verified in section III using simulation data from the Benchmark Target Strength Simulation Submarine (BeTSSi-Sub) model. A scaled (1:20) model is built and used in field experiments to further verify CSPI performance and presented in section IV, analyzing the matching rates and SNRs.

II. Compressive sensing to leverage prior information

A. Principles of Compressive Sensing

The theory of CS states that, as long as a signal is compressible or sparse in a certain transformation domain, a high-dimensional signal can be projected onto a low-dimensional space by a measurement matrix unrelated to the transform base. The original signal can then be reconstructed from a small amount of projections with high probability by solving the optimization problem[12] [13]. The specific process is shown in Fig.1.

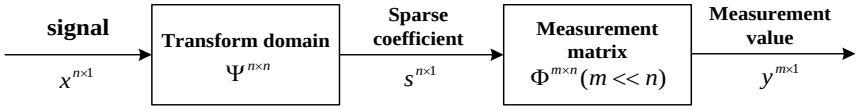

(a) Compressive sensing of signal

(b) Reconstruction of signal

Fig.1 Compressive Sensing (CS) process

Fig.1a shows the linear measurement of sparse signals. Let us consider an N-dimensional and K-sparse signal $x \in R^{n\times1}$. If some orthogonal transformation $\Psi \in R^{n\times n}$ exists, it makes the projection s of x sparse, namely $x^{n\times1} = \Psi^{n\times n} \cdot s^{n\times1}$. It can be projected onto a measurement matrix $\Phi \in R^{m\times n}$ （$m << n$）, which is unrelated to the transformation matrix $\Psi^{n\times n}$, and then one obtains the sample signal $y^{m\times1} = \Phi^{m\times n} x^{n\times1}$. Therefore, this leads to:

$$y^{m\times1} = \Phi^{m\times n} x^{n\times1} = \Phi^{m\times n}\Psi^{n\times n} s^{n\times1} = A^{m\times n} s^{n\times1} \tag{1}$$

where $A \in R^{m\times n}$ is called the sensing matrix.

The CS linear measurement process is non-adaptive, i.e., the measurement matrix Φ does not need to change with the signal x. However, if one wants to perfectly recover the original signal in

a subsequent reconstruction, it requires that the information must not be lost during the measurement. This is achieved using the Restricted Isometry Principle[34] (RIP). When the sensing matrix meets the RIP characteristics, the measurement signal contains all the information necessary to reconstruct the original signal.

The Restricted Isometry Principle (RIP)[34] states that: for any N -dimensional K - sparse signal x, with sparse representation $x = \Psi\theta$. If there is a constant $\varepsilon_{\mathrm{k}} \in (0,1)$, the sensing matrix $A = \Phi\Psi$ satisfies

$$(1-\varepsilon_k)\|\theta\|_2 \le \|A\theta\|_2 \le (1+\varepsilon_k)\|\theta\|_2 \ , \tag{2}$$

it is said that the sensing matrix A satisfies the K -order RIP property, and the constant ε_{k} is called the K -order RIP constant.

However, directly determining whether a matrix satisfies the RIP property is an NP-hard problem. The literature[12] gives an equivalent condition of the RIP property, which is the incoherent principle. When the measurement matrix Φ and the transformation matrix Ψ are incoherent, the sensing matrix $A = \Phi\Psi$ has a great probability to satisfy the RIP property. The incoherence is that the row vectors $\left\{\Phi_i^T\right\}_{\mathrm{j}=1}^{m}$ of the measurement matrix Φ cannot be sparsely represented by the column vectors $\left\{\Psi_i^T\right\}_{\mathrm{j}=1}^{m}$ of the sparse transformation matrix Ψ .

Fig.1b shows the reconstruction process. The n -dimensional original signal x is recovered from the m -dimensional measured value y . Because $m << n$, the inverse problem of equation (1) is an ill-posed problem which cannot be solved. However, if signal x is sparse, the term $s^{n\times 1}$ in equation (1) has only K non-zero coefficients, and as long as it satisfies $m \ge K$, the inverse problem can be solved to obtain the transform sparse signal $s^{n\times 1}$. Research[35] indicates that if there is a $2K$ -order isometry constant $\varepsilon_{2\mathrm{k}} < 1$, which makes the sensing matrix A satisfy the RIP

property, the compression perception problem $y^{m\times1}=\Phi^{m\times n}x^{n\times1}=A^{m\times n}s^{n\times1}$ can be transformed into the following minimum l_0 norm problem:

$$\min\|\mathrm{s}\|_{l_0}\ s.t.As=y \tag{3}$$

However, the minimum l_0 norm solution requires to list all C_n^K possibilities of the non-zero value in s, which is an NP-hard problem. In this case, two methods are used.

One method is to transform the minimum l_0 norm problem into a minimum l_1 norm problem. The literature[34] [36] points out that the solution of the minimum l_0 norm and the minimum l_1 norm problem is equivalent when there exists a $2K$-order isometry constant $\varepsilon_{2\mathrm{k}}<1$, which makes the sensing matrix A satisfy the RIP property. That is to say, the compression perception problem $\mathrm{y}=\Phi x$ can be converted into the following minimum l_1 norm problem:

$$\min\|s\|_{l_1}\ s.t.As=y\ . \tag{4}$$

The minimum l_1 norm problem is also called Basis Pursuit (BP), and the BP algorithms include the interior point method and the gradient projection method.

The other method consists in searching for the secondary optimal solution of the minimum l_0 norm problem. A simple and practical greedy algorithm is presented based on this principle. The greedy algorithms are widely used for compressive sensing signal reconstruction. It allows a certain error ξ to solve the minimum l_0 norm problem:

$$\min\|s\|_{l_0}\ s.t.\|As-y\|<\xi \tag{5}$$

The greedy algorithms commonly used include Matching Pursuit (MP), Orthogonal Matching Pursuit (OMP), and a series of improved algorithms.

In general, the signals we need to process contain noise and interference; the signal that the sensors receive is x:

$$x = \hat{x} + n \tag{6}$$

where x is the signal with noise, $\hat{x}$ is the original signal from the object, n is the noise (including interference). Based on Compressive sensing theory, $\hat{x}$ is the sparse component of x. Atoms are first constructed when x is decomposed and transformed, and the signal properties are related to the atomic properties. Conversely, noise is random without properties. So the reconstructed signal $\hat{x}$ is the original signal of the object and the remaining signal residuals correspond to noise. Therefore, noise can be decreased and SNR improved when the signal is compressed and reconstructed.

B. Prior information

1. Incident signal

The acoustic return from an underwater target is generated by the interaction between incident waves and waves scattered by the target. It contains characteristics of the sonar target, and it also has a close relation with the relative position of the incident waves, the incident sound-wave frequency, and the pulse width. Assuming the target characteristics are linear time invariant, network theory can be used to describe the scattering process. The target is seen as a network system with a transfer function $H(r,\omega)$. The input to the system is the incident plane wave $p_i(r,\omega)$, the output is the scattered signal $p_b(r,\omega)$, and therefore $p_b(r,\omega) = \frac{e^{jkr}}{r} p_i(r,\omega)H(r,\omega)$, where r is the distance between the position of the incident wave and target, ω is the frequency

of sound wave, $k = \omega / c$ is the wave number, and c is the velocity of sound in the water. The scattered signal is the superposition of incident waves with different amplitudes and delays. So the incident signal can be used as a type of prior information.

2. Block-sparse characteristics

Compared to a general sparse signal, a signal is said to be "block-sparse signal" when zero and non-zero value distribution of the signal shows cluster-type characteristics and the non-zero value only appears in certain block positions[37].

The specific form of a block-sparse signal is defined as follows:

$$x = [\underbrace{x_1, \ldots, x_d}_{x^T[1]}, \underbrace{x_{d+1}, \ldots, x_{2d}}_{x^T[2]}, \ldots, \underbrace{x_{n-d+1}, \ldots, x_n}_{x^T[q]}]^T . \quad (7)$$

Where $x[i], i = 1, 2, ..., q$ is a sub-block, for a total of q sub-blocks. In order to simplify the problem, we can assume that $x[i]$ has equal length, the size of each sub-block is d, i.e. the total number of samples is $n = qd$, and x is called as block-sparse signal. When the size of sub-blocks becomes $d = 1$, it becomes a general sparse signal.

According to the of target echo principle given in section II.B.1, the transfer function $H(r, \omega)$ is the main component of the target return, in addition to the incident signal. The highlight model[38] points out that, under the condition of high frequency and limited bandwidth, the returns from an object with complex geometry will be made from the superposition of the sub-target returns. Each sub-target echo can be thought as coming from one particular highlight. The contributions of these highlights are described by three parameters: amplitude factor, delay, and phase jump, so the transfer function of each highlight can be written as $H_i(r, \theta, \psi, \omega) = A_i(r, \theta, \psi) \exp(jw\tau_i) \exp(j\phi_i)$. In this equation, A_i is the amplitude of each

highlight and is related to the distance r and incident angle θ； τ_i is the time delay; ω is the frequency of the signal; and ϕ_i is a random phase.

According to the linear superposition principle, the object is equivalent to the superposition of K highlights, the total transfer function of a model is therefore:

$$H(r,\theta,\psi,\omega)=\sum_{i=1}^{K}A_i(r,\theta,\psi)\exp(jw\tau_i)\exp(j\phi_i) \tag{8}$$

Assuming that the echo highlights are fixed, the echo signal includes K sub-echoes, the echo signal can be expressed as a linear superposition of K sub-echoes according to highlight model(does not consider the influence of phase factors), $x(t)=\sum_{i=1}^{K}A_i s(t-\tau_i)$, $s(t)$ is the incident signal, $x(t)$ is the echo signal, A_i is the amplitudes of sub-echoes.

Therefore, every highlight, every sub-echo, is a "block" of echo signals, the echo signals exhibit a block-sparse feature.

C. Compressive sensing to leverage prior information

The specific process of CSPI is shown in Fig.2.

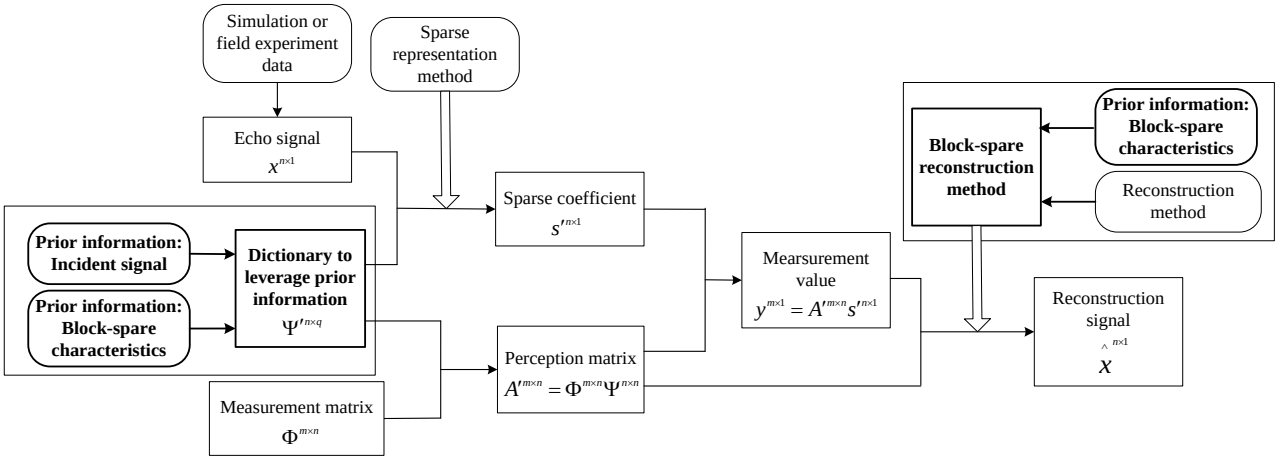

Fig.2 Stages of the CSPI process

The echo signal $x^{n\times1}$ can correspond to a simulation or field test data.

First, the incident signal and block-sparse characteristics are integrated into the construction of a dictionary. The transformation dictionary $\Psi^{n\times n}$, integrating the prior information is formed, and the echo signal $x^{n\times1}$ is decomposed to obtain the sparse coefficient $s^{n\times1}$ using the sparse decomposition method (OMP is used in this paper). The sparse representation process of the signal is then accomplished. This process also proves that the echo signal is indeed sparse and compressible.

At the next stage, the sensing matrix $A^{m\times n}=\Phi^{m\times n}\Psi^{n\times n}$ is formed by the transformation dictionary $\Psi^{n\times n}$ and the measurement matrix $\Phi^{m\times n}$ (a Gaussian measurement matrix is used in this paper). The observed signal $y^{m\times1}=\Phi^{m\times n}x^{n\times1}=\Phi^{m\times n}\Psi^{n\times n}s^{n\times1}=A^{m\times n}s^{n\times1}$ is formed by the measurement matrix $\Phi^{m\times n}$ and the echo signal $x^{n\times1}$. The compression observation process of the signal is then finished.

Finally, the prior information of block sparsity is integrated into the reconstruction algorithm (OMP is used in the paper). The block-sparse OMP reconstruction method is used to reconstruct the compressed signal and obtain the recovered signal $\hat{x}^{n\times1}$.

The realization process of the above CSPI shows that the integration of prior information is mainly reflected at two stages: (1) the formation of the transformation dictionary $\Psi^{n\times n}$ and (2) the reconstruction method of the block-sparse OMP. The following describes this integration of prior information in more details.

1. Dictionary structure using prior information

The key issue in realizing a signal sparse representation is how to construct the sparse dictionary and how to select the suitable atom to represent a signal from the dictionary. The closer

to the original signal the characteristics of the atoms are, the better is the outcomes of compression and reconstruction. Based on the characteristics of the echo and its relation with the incident signal described in section B.1, we will construct the dictionary to leverage prior information with the representation coefficient of the signal only containing a few non-zero elements in the dictionary, achieving the sparse representation of the echo signal. The specific method is described as follows:

The incident and echo signals are sampled at the rate of the Nyquist sampling theorem, and the sampling period is written as T_s. The pulse width of the incident signal is τ, the number of points per pulse width is N, and the total number of sample points is n.

First, the incident signal is discretized and its energy is normalized. The number of sample points per pulse width is N, so this creates an $N \times 1$_dimensional vector s_p. To normalize its energy, we take the 2-norm $\|s_p\|_2 = 1$, resulting in the prototype atom $s_p = [s_p(T_s), s_p(2T_s), ..., s_p(NT_s)]$.

The second stage consists in blocked and shifted processing. According to the principle of the sonar target scattering, the echo wave is formed by the superposition of the incident wave of different amplitudes and delays, so the non-zero support areas of individual atoms in the dictionary have the same waveform features. The distribution of zero and non-zero values in the signal shows cluster properties, and the difference lies in the starting-point coordinates of the non-zero areas. Therefore, we can think of the prototype atom as a block, extend it into $n = M \times N$ points by adding zeroes, make it the same as the number of sample points of the echo, noted as g_1. Taking the different starting points, respectively written as $g_2, g_3, ..., g_n$, this creates the dictionary, which is the transform domain $\Psi^{n \times n} = [g_1^T, g_2^T, ..., g_n^T]^T$ in CS theory. Here,

$$\begin{cases} g_l(i) = s_p, & i \in \{l+1, l+2, ..., l+N\} \\ g_l(i) = 0, & i \in \{1, 2, ..., l\} or \{l+N+1, ..., n\} \end{cases} \tag{9}$$

The non-zero support region of each atom has the same waveform characteristics, and it is consistent with the waveform of the incident signal; the difference lies in the starting point coordinates of the non-zero areas. The dictionary matrix can thus be expressed as

$$\Psi^{n\times n} = \begin{bmatrix} g_{11} & g_{12} & \cdots & g_{1n} \\ g_{21} & g_{22} & \cdots & g_{2n} \\ \vdots & \vdots & \vdots & \vdots \\ g_{n1} & g_{n2} & \cdots & g_{nn} \end{bmatrix} \tag{10}$$

The atoms in the dictionary have the sparse property described in section II.B.2: the zero and non-zero-valued regions appear in the form of blocks. In this paper, the atoms in the dictionary are processed by blocks and each atom is divided into q blocks. For the i -th atom $\mathbf{g_i} = [g_{i1} \quad g_{i2} \quad \cdots \quad g_{in}]$, which can be rewritten as $\mathbf{g_i} = \left[\underbrace{g_{i1}, \cdots, g_{id}}_{\mathbf{g'_{i1}}}, \cdots, \underbrace{g_{n-d+1}, \cdots, g_n}_{\mathbf{g'_{iq}}} \right]$. Dividing into q blocks, this becomes $\mathbf{g'_i} = \left[\mathbf{g'_{i1}} \quad \mathbf{g'_{i2}} \quad \cdots \quad \mathbf{g'_{iq}} \right]$. So, after the dictionary is blocked, it is changed into $\Psi' = \left[\mathbf{g'_1}^T \quad \mathbf{g'_2}^T \quad \cdots \quad \mathbf{g'_n}^T \right]^T$. In other words, $\Psi^{n\times n}$ becomes $\Psi'^{n\times q}$, where $q < n$.

2. Signal reconstruction using prior information

Traditional sparse-signal reconstruction methods generally address random sparse signals; non-zero element positions in the signal randomly appear, and the specific characteristics of the signal are not considered. In the present case, we can use the prior information about how the incident wave influences target echoes. We decided to use the Orthogonal Matching Pursuit (OMP)

method, integrating the block-sparse characteristics into the reconstruction algorithm and achieving the purpose from single-point matching to block matching.

The main idea of OMP[39][40] is to use a greedy iterative way, selecting the most relevant column of the sensor matrix A from the compressed observation signal y, subtracting its projection onto the column from the observation signal, thus obtaining a residual signal. We can then continue to select the column most relevant to the residual signal. This process repeats until the energy of the residual signal is less than the given threshold or the algorithm reaches other termination conditions.

The specific implementation process is as follows:

（1）Initialize $r_0 = y$， $\Lambda_0 = \Phi, A_0 = \Phi$， $i = 1$；

（2）Find index λ_i, make $\lambda_i = \arg\max_{j=1,2,\ldots,n} \left[\left\langle r_{i-1}, \alpha_j \right\rangle \right]$；

（3）Store the matching point information， $\Lambda_i = \Lambda_{i-1} \cup \{\lambda_i\}$， $A_i = A_{i-1} \cup \left\{ a_{\lambda_i} \right\}$；

（4）Find the least-squares solution of $y = A_i s_i$： $\hat{s}_i = \arg\min_{s_i} \| y - A_i s_i \| = (A_i^T A_i)^{-1} A_i^T y$；

（5）Update the residual $r_i = y - A_i \hat{s}_i = y - A_i (A_i^T A_i)^{-1} A_i^T y$；

（6）Iterate: $i = i + 1$, if $i \le K$ return to step (2), otherwise stop iterating and move to step (7);

（7）After obtaining $\hat{s}$, the reconstructed signal $\hat{x} = \Psi \hat{s}$ can be obtained using a transformation matrix (dictionary).

In the above process, r_i represents the residual， i represents the iterations number， Φ represents an empty set， Λ_i represents the index (column number) set of the i th iteration, λ_i

represents the index (column number) of the i th iteration, α_j represents the column j of matrix A, A_i represents the set of columns of the matrix A selected by index Λ_i, s_i is a column vector of $i\times 1$, $\cup$ represents the set union, and $\langle \bullet, \bullet \rangle$ represents the inner product of the vector.

We can see from step (6) that the number of iterations of the OMP algorithm is the signal (point) sparsity K: the number of non-zero values in the signal is the number to match. After each match, we find a sample point, which destroys the block-sparse structure of the signal and affects the reconstruction effect. At the same time, the calculation efficiency will decrease when the non-zero point is further increased.

In this paper, we consider the blocking characteristics of the echo signals[41]: the echo signals and dictionary are both blocked and we find the best matching blocks one by one. The integration process of the block-sparse prior information is the following. The sensing matrix is blocked as $A=[\underbrace{A_1,\cdots,A_d}_{A^T[1]},\underbrace{A_{d+1},\cdots,A_{2d}}_{A^T[2]},\underbrace{A_{n-d+1},\cdots,A_n}_{A^T[q]}]^T$ based on the block dictionary $\Psi'^{n\times q}$ formed in 1, and then, we search the most relevant columns of the observed signal with sensing matrices by block matching, and store the column information. We search a block of the echo signal, rather than a point. The number of iterations is the block sparsity of the echo signal.

The specific realization process is described as follows:

（1）Initialize $r_0 = y$， $\Lambda_0 = \Phi$， $A_0 = \Phi$， $i = 1$；

（2）Find set of index λ_i， make $\lambda_i = \arg\max_{j=1,2,\ldots,n} \left[\left\langle r_{i-1}, \alpha_j \right\rangle \right]$；

（3）Store support block set information， $\Lambda_i = \Lambda_{i-1} \cup \{\lambda_i\}$， $A_i = A_{i-1} \cup \{a_{\lambda_i}\}$；

（4）Find the least-squares solution of $y = A_i s_i$： $\hat{s}_i = \arg\min_{s_i} \|y - A_i s_i\| = (A_i^T A_i)^{-1} A_i^T y$；

（5）Update the residual $r_i = y - A_i \hat{s}_i = y - A_i (A_i^T A_i)^{-1} A_i^T y$;

（6）Iterate: $i = i + 1$, if $i \le K'$ return to step (2), otherwise stop iterating and move to step (7);

（7）After obtaining $\hat{s}$, the reconstructed signal $\hat{x} = \Psi \hat{s}$ can be obtained by using a transformation matrix (dictionary).

For the above realization process, we can see that the processes of Block OMP (BOMP) and OMP are basically similar, and the differences lie mainly in steps (2), (3), and (6). In step (2), the OMP method finds the largest point of the inner product, with the point best matching the observed signal; whereas the BOMP method finds a block best matching the observed signal. In step (3), the OMP method stores the matching point information; whereas BOMP stores the support block set information. And in step (6), the sparsity of the OMP method is the number of non-zero points; whereas that of the BOMP method is the number of non-zero blocks.

III. Verification of CSPI using simulation data

A. Target and simulation model

The target selected for this investigation is a scaled (1:20) model of the Benchmark Target Strength Simulation Submarine (BeTSSi-Sub), which corresponds to a specific, real submarine. It was designed and developed by FWG (Forschungsanstalt der Bundeswehr für Wasserschall und Geophysik) in Germany, in order to compare the prediction and test the performance of different methods. Fig.3 shows the dimensions of the scaled BeTssi-Sub model. The scaled length is 3 m, the distance between the bow and the bridge is 1.2 m, the diameter of the entire body is 0.35 m and the diameter of the bridge is 0.525 m. The incident angle θ refers to the angle between the incident signal and the bow direction.

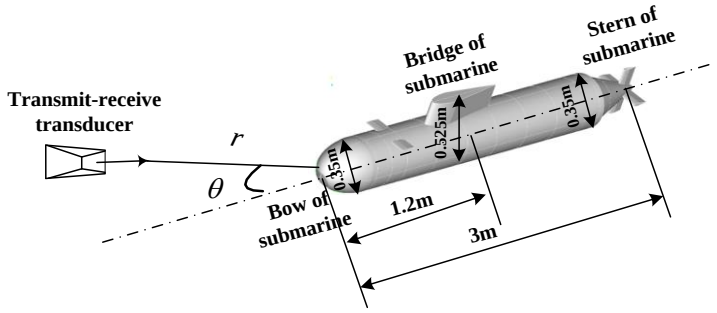

Fig.3 Scaled BeTssi-Sub model

The major contributions of submarine scattering will unsurprisingly come from the main elements of the bow, bridge, and stern, so we approximate the submarine as three rigid spheres, representing each of these three parts and with a diameter equal to their respective sizes (shown in Fig.3). Each sphere has a distinct scattering strength, noted respectively as relative value $b_1 = 0.2$ (bow), $b_2 = 0.3$ (bridge), and $b_3 = 0.2$ (stern).

B. Echo simulation - method and results

According to the principle of sonar target echo given in section II.B, the total transfer function of a model with three-highlight is therefore:

$$H(r,\theta,\psi,\omega) = \sum_{i=1}^{3} A_i(r,\theta,\psi)\exp(jw\tau_i)\exp(j\phi_i) \tag{11}$$

The magnitude of the echo wave is obtained by calculating the target strength of each highlight[42], as follows:

$$TS_i(\theta) = 10\log(r^2/4) + 10\log(b_i), \quad A_i = 10^{TS_i(\theta)/20} \tag{12}$$

According to the geometric relations shown in Fig.3, the time delay of the i-th highlight is

$$\tau_i = 2\sqrt{(r + L_i\cos\theta)^2 + \frac{(L_i\sin\theta)^2}{c}} \tag{13}$$

where r is the distance between the transducer and the bow, θ is the incident angle, and L_i

is the distance between the highlight and the bow.

The incident signal is given as $p_i(t) = p_0(t)\exp(-j\omega t)$, with p_0 being the trapezoidal single-frequency pulse signal. The centre frequency of the incident signal is selected as $\omega = 40kHz$, the distance from the transmitting signal to the target as $r = 20m$ and sound velocity is chosen as $c = 1500m/s$. The echo signal is represented as $p_b(t) = \sum_{i=1}^{3} A_i\, p_0(t-\tau_i)\exp[j\omega(t-\tau_i)]\exp(j\phi_i)$.

The waveforms of different incident angles are shown in Fig.4. When $\theta = 30^o$, the distance difference between the incident signal and the three highlights is greater than one pulse width; the three highlights are completely separated. As the incident angle increases, the distance difference is getting increasing smaller, and the three highlights become gradually closer ($\theta = 60^o$). When $\theta = 90^o$, the distance difference is so small that the three highlights are now superimposed.

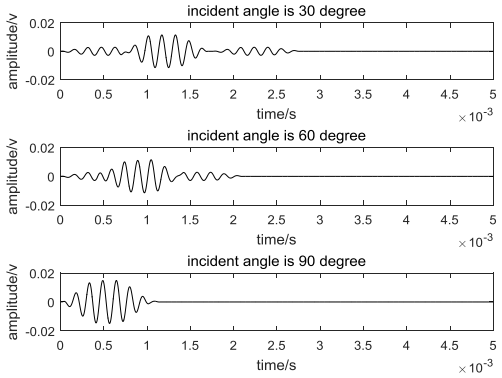

Fig.4 Waveform of echo signal for different incident angles

C. Verification of the performance of CSPI for simulation data

1. Evaluation parameters

To verify the performance of the CSPI approach, we use the following formulae to calculate the matching rate (measuring the similarity between two signals) and the SNR (proportional relationship between the active component and the noise component in the signal)[43].

$$Matching\_rate = 1 - \left(\left\| \hat{X}' - X' \right\|_2 / \left\| \hat{X}' + X' \right\|_2 \right) \tag{14}$$

$$SNR = 10\lg(\left\| \hat{X} \right\|_2^2 / \left\| X - \hat{X} \right\|_2^2) \tag{15}$$

In which X is the original signal, $\hat{X}$ is the reconstruction result, and X' and $\hat{X}'$, respectively, represent the absolute values of X and $\hat{X}$.

2. Reconstruction results for simulation data

We compare the results of CSPI with CSDCT (the sparse matrix is discrete cosine transformation without prior information). First, we extract a small amount of data with a Gaussian random measurement matrix, and then reconstruct the signal by using CSPI and CSDCT, respectively. The reconstruction results are shown in Fig.5. Fig.5 (a) shows the results for an echo signal without noise, with a compression ratio of 5% (i.e. extracting 5% of data volume). Fig.5 (b) shows the results for an echo signal with noise (SNR = 4dB), with a compression ratio of 5%. Fig.5 (c) shows the results for an echo signal with noise (SNR = 0dB), with a compression ratio of 40%.

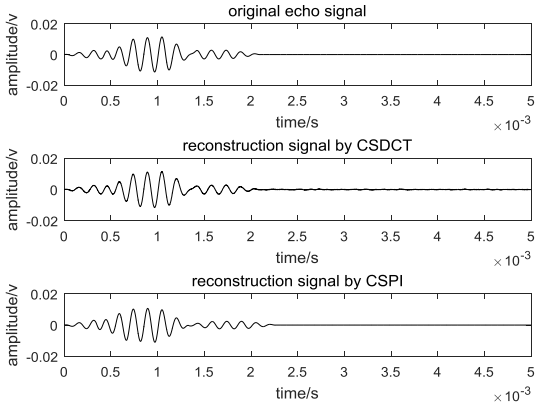

(a) Signal without noise (compression ratio is 5%)

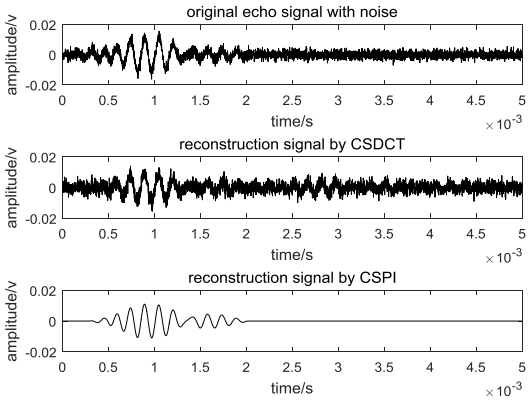

(b) Signal with noise (SNR is 4dB, compression ratio is 5%)

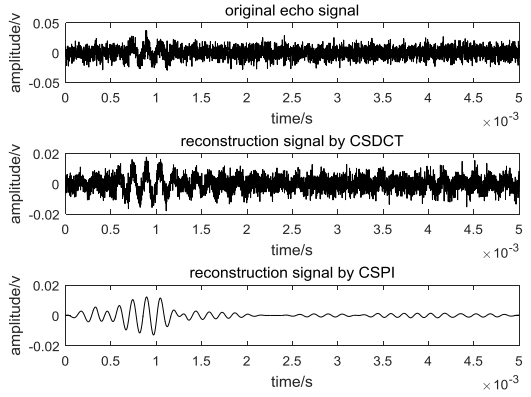

(c) Signal with noise (SNR is 0dB, compression ratio is 40%)

Fig.5 Reconstruction results

From Fig.5, we can see that for the echo signal without noise, CSPI and CSDCT can reconstruct the original signal perfectly using only a small amount of data, but as noise becomes important, CSPI clearly gives superior results. When the SNR equals 4dB, CSPI can not only reconstruct the original signal but also greatly reduce the noise. When the SNR reaches 0dB, the signal is almost invisible, but CSPI can still reconstruct the main signal. The results show the performance of CSPI to improve SNR.

3. Reconstruction accuracy analysis

We evaluate the performance of CSPI in terms of compression, reconstruction, and SNR improvement through the relation among matching rate, SNR, and compression ratio.

(1) The performance in terms of compression and reconstruction - Matching rate

Fig.6 shows the relation between matching rate and compression ratio. Fig.6 (a) shows the result for the signal without noise; we can see that the matching rates of CSPI and CSDCT are both close to 1 when the compression ratio is more than 5%, which indicates that they can reconstruct the original signal almost perfectly. Fig.6 (b) shows the result for the signal with noise (SNR = 4dB), where the three lines, respectively, represent the matching rate of the original signal, the reconstruction signal by CSPI, and that by CSDCT. We can see that when the compression ratio is more than 3%, the CSPI approach can obtain the same matching rate as the original signal, and with an increasing in the compression ratio, the matching rate of CSPI can reach about 0.95; thus, CSPI performs better than CSDCT. Fig.6 (c) shows the result for the signal with high noise (SNR = 0dB): the signal is then very weak, and the matching rate of the original signal is less than 0.3, but that of CSPI can still reach about 0.8. Fig.6 shows the performance of CSPI in compression and reconstruction.

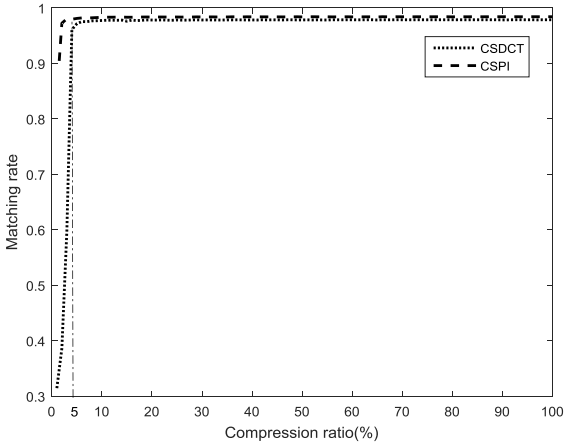

(a) Signal without noise

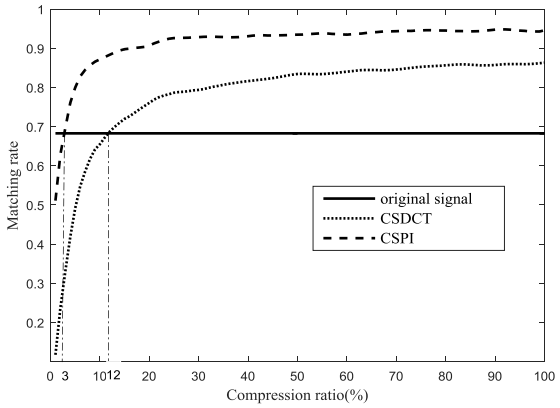

(b) Signal with noise (SNR=4dB)

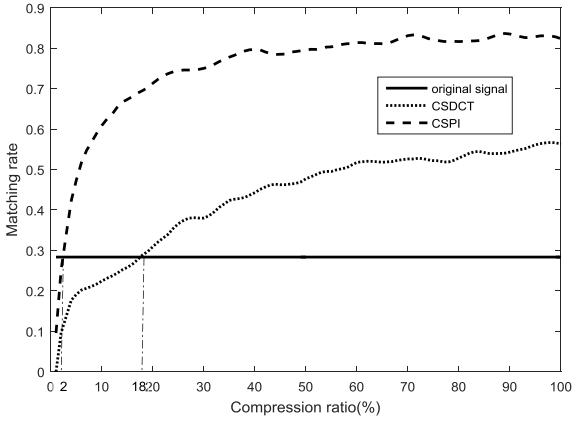

(c) Signal with noise (SNR=0dB)

Fig.6 Variation in matching rate with compression ratio

(2) Performance in terms of SNR improvement

Fig.7 shows the relation between SNR and compression ratio. Fig.7 (a) shows the result for the signal with SNR = 4dB, and we can see that CSPI can obtain the same SNR using 2% data and 17dB SNR using 30% data; that is, CSPI can improve SNR by 13dB using 30% data. Fig.7 (b) shows the results for the weak signal SNR = 0dB: CSPI still works very well and can improve the SNR by 7dB using 32% data. Fig.7 shows the performance of CSPI in improving the SNR.

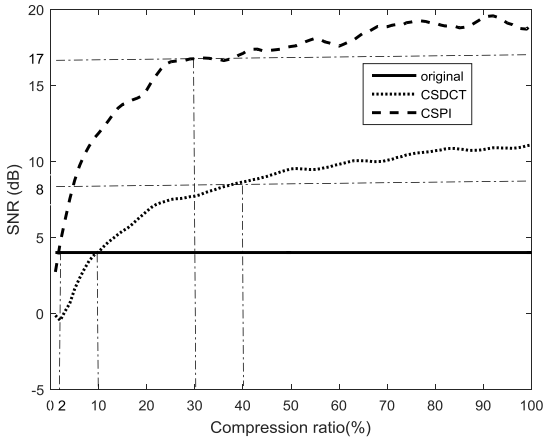

(a) Signal of SNR = 4dB

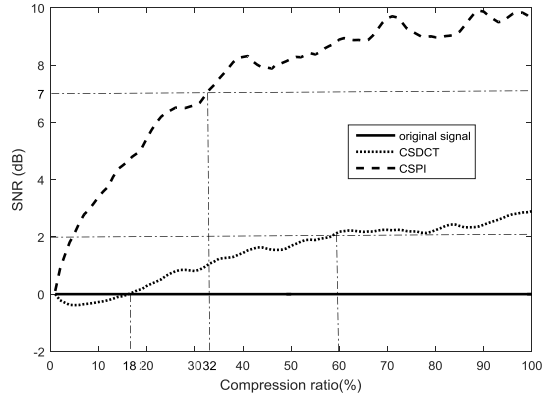

(b) Signal of SNR = 0dB

Fig.7 Variation in SNR with compression ratio

IV. Verification of CSPI using field experiment data

A. Summary of field experiments

The test was carried out at the experimental station of Qiandao Lake, a human-made, freshwater lake located in Chun'an County, Zhejiang Province, China. The test target is the 1:20 scaled model of the BeTSSi-Sub (described in section III A). The deployment method is shown in Fig.8. There are two rotation devices, one for the transmitting and receiving transducer (working at 40-80kHz) and one for the rig holding the model submarine. They are 20 m apart, and both are

10 m underwater. In order to obtain echo signals at different incident angles, the submarine model is rotated counterclockwise at uniform velocity.

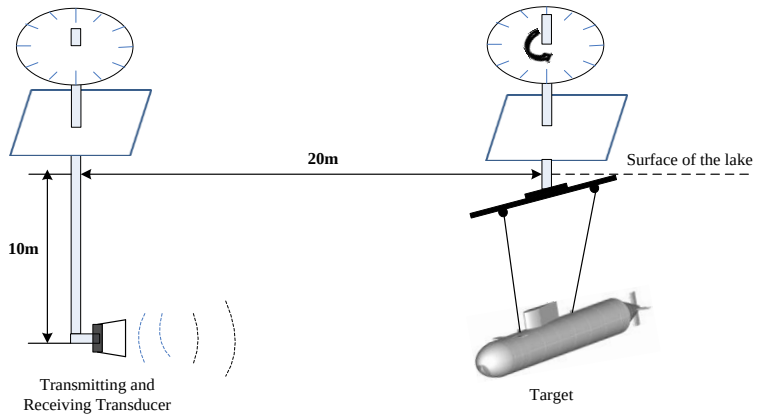

Fig.8 Deployment method of the test

B. Backscattering measurements

In the experiment, the object was rotated counterclockwise at uniform velocity. Echo signals were obtained with different incident angles. From the entire dataset, we selected the echo signals corresponding to the same incident angles of 30^{o}, 60^{o}, and 90^{o}, as shown in Fig.9.

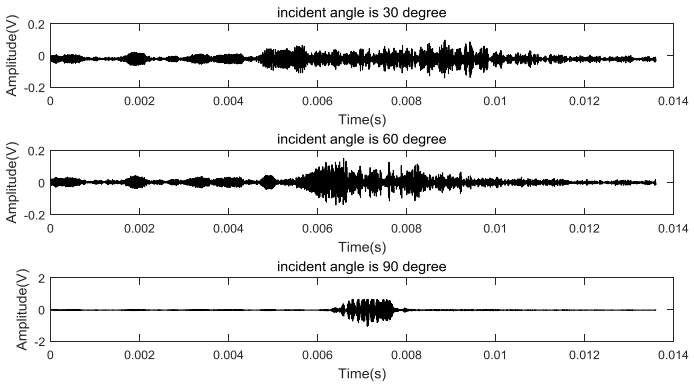

Fig.9 Backscatter echoes from the scaled submarine model at different incidence angles

C. Verification of the performance of CSPI for field experiment data

For a first illustration of the CSPI process, we present the signals at the incident angle of 60^{o}, comparing the original signal with its reconstructions with CSDCT and CSPI with a compression ratio of 20% (Fig.10).

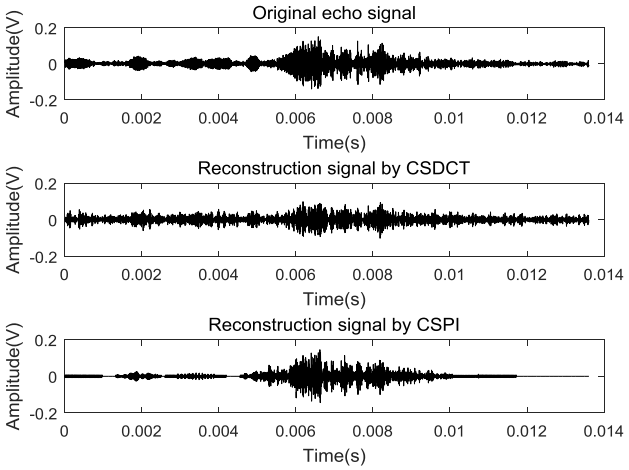

Fig.10 Comparison of original signal with its reconstruction with the CSDCT and CSPI approaches

To verify the performance of CSPI in improving SNR, illustrated here for the signal at incident angle 60^{o}, we plot the variation of SNR with the compression ratio (Fig.11).

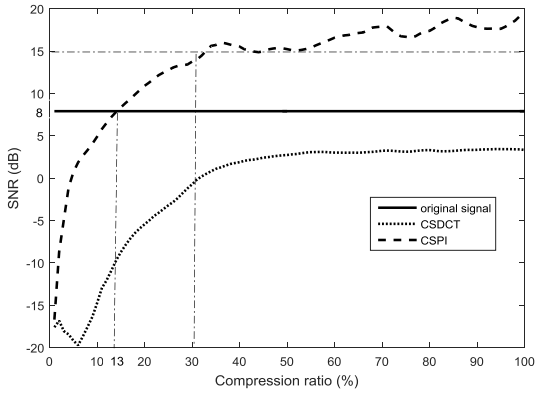

Fig.11 Variation of SNR with compression ratio for incident angle of 60^{o}

From the above curve, we can see that the SNR of the original signal is 8dB, and it can be improved by CSPI using 13% data. If we use 30% data, we can obtain a 15dB SNR, i.e. the SNR

can be improved by 7dB. With the increasing of the compression ratio, CSPI increases SNR again. But because of the influence of interference, the performance of CSDCT visibly declines.

The field measurements are affected by other types of interference in addition to noise and the test system itself, such as false target, reverberation from the surface of the water, the bottom of the lake and other objects further away. Compression sensing methods reconstruct the signals by matching them to the atoms in the dictionary, and suppress the noise by signal and atoms correlation, and noise and atoms non-correlation, thereby improving SNR. However, echoes from false targets and the reverberation from surface and bottom of water are also caused by the scattering, and these kinds of scattering waves will also match the atoms, especially when the object echoes are very weak, it will have a more serious impact on the real target echo. Therefore, the field test results might not always be as good as the simulation results, but their successful reconstruction again fully reflects the advantages of CSPI method proposed in this paper.

V. Conclusions

The processing of acoustic returns from objects imaged with an active sonar can make use of some prior information. Combining the prior information and CS theory, we present the CSPI approach and illustrate its use with both simulation data and a field experiment. The CSPI has clear advantages. It reduces the data needed to reconstruct the echo of a known signal and significantly improves matching rates and SNR.

Simulating the echoes from the BeTSSi-Sub model without noise, CSPI can accurately reconstruct the echo signal using less data (5% here), with a matching rate close to 1. When there is noise in the echo signal, CSPI can significantly decrease the noise, and better reconstruct the original signal. When SNR = 4 dB, CSPI can improve the SNR by 13 dB to 17 dB using 30% data, and with the increasing of the compression ratio, SNR can be improved further. When SNR = 0

dB, the echo signal is almost invisible, detection and recognition are very difficult, but CSPI can still reconstruct the echo signal and improve SNR to more than 7 dB. For field experiment data obtained in a large freshwater lake with noises and other interferences, CSPI can improve the SNR when the compression ratio is greater than 13%. When the compression ratio if more than 30%, the SNR can reach 15 dB, and with the increasing of compression ratio, we can obtain increased SNR.

From the verification results for the simulation signal and field experiment data, we can see that CSPI can not only reduce the data volume but also improve SNR. The combination of Compressive Sensing with Prior Information presented in this paper can provide an effective path for active sonar detection and recognition of weakly scattering underwater targets and small signals buried in important noise.

Acknowledgments: This article uses experimental data collected at Dalian Test & Control Institute (China), and we gratefully acknowledge our colleagues for their experimental skills. T. Sun wrote this article as a Visiting Research Fellow to the University of Bath (UK), thanks to the Chinese Scholarship Council (State Scholarship Fund No. 201608330338). The article is also supported by Pre-research field fund project from Chinese Military Equipment Development Department (No. 6140243010116DZ04001).

References

[1]A. M. Gunderson and P. L. Marston, "Kirchhoff approximation for backscattering from a partially exposed rigid sphere at a flat interface," J. Acoust. Soc. Am. 140(5), 3582-3592(2016).

[2]C. He, A. Zhao, B. Zhou, X. Song, and F. Niu, "Parameter measurement research of sonar echo highlights," J. Acoust. Soc. Am. 135(4), 2303-2303 (2014)

[3]Y. H. Ji, G. H. Byun, J. S. Kim, and H. S. Bae, "Multi-static scattering characteristics of

submerged objects with experimental investigation," J. Acoust. Soc. Am. 134(5), 4113-4113 (2013).

[4]A. M. Padilla, K. M. Rychert, and T. C. Weber, "Experimental observations of acoustic backscattering from spherical and wobbly bubbles," J. Acoust. Soc. Am. 141(5), 3607-3607(2017).

[5]K. Zhao, J. Liang, J. Karlsson, and J. Li, "Enhanced multistatic active sonar signal processing," J. Acoust. Soc. Am. 134(1), 300-311 (2013).

[6]B. M. Worthmann and D. R. Dowling, "Target localization in a reverberant shallow ocean waveguide with environmental uncertainty using a nonlinear frequency-difference signal processing technique," J. Acoust. Soc. Am. 139(4), 2196-2196(2016).

[7]D. Chu and G. Eastland, "Calibration of a broadband acoustic transducer with a standard spherical target in the near field," J. Acoust. Soc. Am. 137(4), 2148-2157 (2015).

[8]F. Wang, S. Du, W. Sun, Q. Huang, and J. Su, "A method of velocity estimation using composite hyperbolic frequency-modulated signals in active sonar," J. Acoust. Soc. Am. 141(5), 3117 (2017).

[9]H. Lew, "Broadband echoes from underwater targets," International Journal of Computational Engineering Science, 5(2), 281-290(2004).

[10]B. Jones, T. K. Stanton, J. A. Colosi, R. C. Gauss, J. M. Fialkowski, and J. M. Jech, "Broadband classification and statistics of long-range, mid-frequency sonar measurements of aggregations of fish," J. Acoust. Soc. Am. 135(4), 2152 (2014)

[11]C. F. Gaumond, "Information transfer of broadband sonar echoes," J. Acoust. Soc. Am. 134(5), 4112 (2013).

[12]D. L. Donoho, "Compressed sensing," IEEE Transactions on Information Theory, 52(4), 1289-1306(2006).

[13]E. J. Candès, "Compressed sampling," Proceedings of the International Congress of

Mathematicians (Madrid, Spain), 3, 1433-1452(2006).

[14]E. J. Candès, J. K. Romberg, and T. Tao, "Robust uncertainty principles: Exact signal reconstruction from highly incomplete frequency information," IEEE Transactions on Information Theory, 52(2), 489-509(2006).

[15]E. Lin, C. I. Henry Chen, L. L. Liou, and D. M. Lin, "Performance analysis of digital wideband receiver based on reconstruction of Compressed sensing data," IEEE Rader Conference, 0830 – 0835(2017).

[16]X. Wang, H. Wang, X. Zeng, K. Guo, and J. Sun, "Broadband Compressive Sampling with Deterministic Measurement Matrix," Communications Technology, 48(10), 1111-1115(2015).

[17]M. Lustig, D. Donoho, and J. M. Pauly, "Sparse MRI: The application of compressed sensing for rapid MR imaging," Magnetic Resonance in Medicine, 58(6), 1182-1195(2007).

[18]J. Ma, L. Ge, H. Yuan, and T. Zhang, "Sparse MRI reconstruction based on L_(1/2) regularization," Journal of Hebei University of Technology, 44(4), 1-8(2015).

[19]S. L. Keeling, C. Clason, M. Hintermüller, F. Knoll, A. Laurain, and G. von Winckel, "An image space approach to Cartesian based parallel MR imaging with total variation regularization," Medical Image Analysis, 16(1), 189-200(2012).

[20]M. A. Herman, T. Strohmer, "High-Resolution Radar via Compressed Sensing," IEEE Transactions on Signal Processing, 57(6), 2275-2284(2008).

[21]N. Whitelonis and H. Ling, "High-Resolution Radar Imaging Through a Pipe Via MUSIC and Compressed Sensing," Antennas & Propagation IEEE Transactions on, 61(6), 3252-3260(2013).

[22]S. S. Ram and A. Majumdar, "High-resolution radar imaging of moving humans using doppler processing and compressed sensing," IEEE Transactions on Aerospace & Electronic Systems, 51(2), 1279-1287(2015).

[23]Z. Qin, Y. Liu, and Y. Gao, "Wireless Powered Cognitive Radio Networks With Compressive Sensing and Matrix Completion," IEEE Transactions on Communications, 65(4), 1464-1476(2017).

[24]W. U. Bajwa, J. D. Haupt, and A. M. Sayeed, "Joint Source-Channel Communication for Distributed Estimation in Sensor Networks," IEEE Transactions on Information Theory, 53(10), 3629-3653(2007).

[25]Z. Xie and D. J. Klionsky, "Joint SNR and channel estimation for 60 GHz systems using compressed sensing," IEEE Wireless Communications and NETWORKING Conference, 2896-2901(2013).

[26]P. Li and Y. Yang, "Compressed sensing based acoustic data compression and reconstruction technology," Technical Acoustics, 33(1), 14-20(2014).

[27]G. F. Edelmann and C. F. Gaumond, "Beamforming using compressive sensing," J. Acoust. Soc. Am., 130(4), 232-237 (2011).

[28]A. Xenaki and P. GerstoftKlaus, "Compressive beamforming," J. Acoust. Soc. Am. 136(5), 260-260 (2014).

[29]R. Menon and P. Gerstoft, "High resolution beamforming using L1 minimization," Proc. Mtgs. Acoust. 19, 070091 (2013)

[30]N. Sabna, M. H. Supriya, and P.R. S. Pillai, "Computationally Efficient Sparse Reconstruction of Underwater Signals," Proceeding of Sympol, 88-95(2013).

[31]M. Liao, X. Zhang, and X. Zhang, "Classification and Recognition of Underwater Acoustic Signal Based on Sparse Representation," Journal of Detection & Control, 36(4), 67-77(2014).

[32] B. Yang, Y. Bu, and H. Zhao, "Features of underwater echo extraction based on signal sparse decomposition," Acta Acustica, 35(6), 608-614(2010).

[33]J. F. C. Mota, N. Deligiannis, and M. R. D. Rodrigues, "Compressed Sensing With Prior Information: Strategies, Geometry, and Bounds," IEEE Transaction on Information Theory, 63(7), 4472-4496 (2017).

[34]E. Candès, "Near optimal signal recovery from random projections: Universal encoding strategies," IEEE Trans. Inform. Theory, 52(12), 5406-5425(2006).

[35]E. Candès, and M. Wakin, "An introduction to compressive sampling," IEEE Signal Processing Magazine, 21-30 (2008).

[36] E. Candès, "The restricted isometry property and its implications for compressed sensing," C.R. Math. Acad. Sci. (Paris), 346(9), 589-592 (2008).

[37]M. F. Duarte and Y. C. Eldar, "Structured compressed sensing: from theory to applications," IEEE Transaction on Signal Processing, 4053-4085 (2011).

[38]W. Tang, "Highlight model of echoes from sonar targets," Acta Acustica, 19(2), 92-100 (1994).

[39]S. Mallat and Z. Zhang, "Matching pursuits with time-frequency dictionaries," IEEE Transactions on Signal Processing, 41(12), 3397-3415 (1993).

[40]J. Tropp and A. Gilbert, "Signal recovery from random measurement via orthogonal matching pursuit," Trans. Inform. Theory, 53(12), 4655-4666 (2007).

[41]Y. C. Eldar, P. Kuppinger, and H. Blcskei, "Block-sparse signals: uncertainty relations and efficient recovery," IEEE Transactions on Signal Processing, 58(6), 3042-3054 (2010).

[42]S. Chen, Z. Xie, and Y. Yu, "Simulation of Simplified Reflect Highlights Model from Submarine," Audio Engineering, 35(7), 53-55 (2011).

[43]Q. Ma, "Research on Signal Reconstruction Algorithms for Compressed Sensing," Master's thesis of Nanjing University of Posts and Telecommunications, 12-13 (2013).